Clinics of Oncology

Research Article ISSN: 2640-1037 | Volume 6

Identification of the Enrichment Pathways of Catalase in Multiple Primary Tumors

Chen PM[1] and Chu PY[2,3,4*]

[1]Research Assistant Centre, Show Chwan Memorial Hospital, Changhua 500, Taiwan

[2]Department of Post-Baccalaureate Medicine, College of Medicine, National Chung Hsing University, Taichung, 402, Taiwan

[3]Department of Pathology, Show Chwan Memorial Hospital, Changhua 500, Taiwan

[4]National Institute of Cancer Research, National Health Research Institutes, Tainan 704, Taiwan

[*]Corresponding author:

Pei-Yi Chu,
Department of Post-Baccalaureate Medicine and Pathology, College of Medicine, National Chung Hsing University, Show Chwan Memorial Hospital, National Health Research Institutes, Taiwan,
Tel: +886-4-7256166;
E-mail: chu.peiyi@msa.hinet.net

Received: 15 Sep 2022
Accepted: 01 Oct 2022
Published: 07 Oct 2022
J Short Name: COO

Keywords:

ROS; SOD2; CAT; TCGA

Citation:

Chu PY. Identification of the Enrichment Pathways of Catalase in Multiple Primary Tumors. Clin Onco. 2022; 6(12): 1-10

1. Abstract

1.1. Background: Reactive oxygen species (ROS) has been detected in almost all cancers, which it involves many aspects of carcinogenesis and tumor progression. We previously reported a novel oncogenic role of manganese superoxide dismutase (MnSOD; SOD2) in invasive lung adenocarcinoma (LUAD) by upregulating forkhead box protein M1 (FOXM1) and matrix metalloproteinase-2 (MMP2) expression. In this study, we used a comprehensive analysis and further evaluated the effects of a hydrogen peroxide (H2O2) scavenger, catalase (CAT) in The Cancer Genome Atlas (TCGA) datasets of the different cancer types.

1.2. Methods: A panel gradual increases invasive cell lines were investigated to determine if CAT expression could be changed. Comparison of CAT expression in normal tissues and tumors was analyzed and Kaplan Meier survival analysis for CAT expression in the thirty-three cancer types from TCGA datasets. We also further analyzed the CAT correlated differentially expressed genes (DEGs) in these datasets by the Kyoto Encyclopedia of Genes and Genomes (KEGG) of gene set enrichment analysis (GSEA). We screened out common genes of each pathway as a signature that represented its pathway for Kaplan Meier survival analysis.

1.3. Results: High CAT expression was correlated with low invasiveness in LUAD. High CAT expression had better prognosis in BLCA, KIRC, LIHC, and LUAD, which associated with six enrichment pathways, the upregulation of butanoate metabolism, fatty acid degradation, PPAR signalling pathway, propanoate metabolism, valine, and leucine and isoleucine degradation and the downregulation of DNA replication. By the inductive reasoning, high propanoate metabolism had better prognosis in BLCA, high butanoate metabolism, fatty acid degradation, PPAR signalling pathway, valine, and leucine and isoleucine degradation had better prognosis in KIRC, and high fatty acid degradation had better prognosis in LIHC, whereas high DNA replication had worse prognosis in LUAD.

1.4. Conclusions: Overall, our findings reveal an opportunity for CAT and its associated enrichment metabolic pathways, as dietary therapeutic modalities against metastatic BLCA, KIRC, LIHC, and LUAD.

2. Introduction

Cancer ranks as a leading cause of death and a menace to life expectancy, and a 47% rise of the global cancer will increase 28.4 million cases from 2020 to 2040 due to demographic changes [1]. Reactive oxygen species (ROS) have been generally explored in various human diseases, including cancers [2, 3].

In mitochondria, superoxide anion (O2) is produced as an unavoidable byproduct of electron transport chain during oxidative phosphorylation for ATP synthase [2].

About 80% superoxide anion is generated at complexes I and III and released into the intermembrane space of mitochondria and about 20% superoxide anion is generated the mitochondrial matrix [4].

The manganese superoxide dismutase (MnSOD; SOD2) is an important antioxidant enzyme in the mitochondria to detoxify free radical O2 generated by mitochondria respiration into hydrogen peroxide (H2O2) (Figure1A) [5-8]. Among the reactive oxygen species (ROS), O2 has been postulated to be a key metabolite for the induction of ferroptosis in human cancers [9] and H2O2 is a main second messenger involved in various oncogenic signal transduction pathways and tumor progression [10-12]. Our previous and others have been revealed SOD2 overexpression enhances tumor invasiveness, drug resistance, and clinical prognosis by different mechanisms in lung adenocarcinoma (LUAD) [13-18].

Catalase (CAT), a tetrameric enzyme with four tightly bound molecules of nicotinamide adenine dinucleotide phosphate (NADPH) which catalyze neutralize the noxious H2O2 to oxidane (H2O) and molecular oxygen (O2) (Figure1A), are important members of the antioxidant defense system of cells of almost all aerobic organisms [19-21]. CAT overexpression decreased HBx expression from HBV genome to depressed HCC proliferation and had a better prognosis in liver hepatocellular carcinoma (LIHC) [22]. In a previous study, CAT expression decreased H2O2 level and inhibited cell invasion and migration of lung cancer cells, but its clinical prognosis of LUAD was unveiled [23]. Conversely, CAT overexpression markedly increased anchorage-independent colony formation, acted as a hallmark of the aggressive phenotype, and resisted to temozolomide (TMZ) and radiation in Glioblastoma multiforme (GBM) [24].

However, the role of CAT in tumor progression associated the precise molecular pathways is not fully elucidated, which could assist in developing new methods for the diagnosis and therapy.

With the advances in high throughput gene expression analysis by next generation sequencing (NGS) technology that will be unveiled the effects of well-characterized signaling pathways on clinical prognosis. In this study, we first examined SOD2 and CAT in a series of human lung adenocarcinoma cells with different invasive ability that derived from CL1 cells. Based on TCGA datasets, we performed Kaplan-Meier survival analysis to identify CAT expression had a prognostic signature for overall survival (OS) in BLCA, KIRC, LIHC, and LUAD. We further inputted CAT correlated the differentially expressed genes (DEGs) of BLCA, KIRC, LIHC, and LUAD into a gene set enrichment analysis (GSEA) software for Kyoto Encyclopedia of Genes and Genomes (KEGG) pathways were conducted, and the enrichment pathways and enrichment-related genes of BLCA, KIRC, LIHC, and LUAD were intersected using Venn diagram for the further prognosis analysis.

Based on bioinformatics, we used an in-silico analysis with ALLGGEN_PROMO to predict a large number of FOXO3 binding sites in the CAT promoter region.

3. Materials and Methods

3.1. Cell Culture

CL1-0, CL1-1, CL1-3 and CL1-5 cells were cultured in RPMI-1640 medium contained 10% FBS supplemented with penicillin (100 U/ml) and streptomycin (100 mg/ml). The CL1-0, CL1-1, CL1-3, CL1-5 and CL3 cells were kindly provided by Dr. Pan-Chyr Yang (Department of Internal Medicine, National Taiwan University College of Medicine). Cells were grown at 37℃ in a humidified incubator at 5% CO2.

3.2. Western Blot Analysis

Proteins from CL1-0, CL1-1, CL1-3 and CL1-5 cells were extracted and separated by 10% SDS–PAGE before transferring to a nitrocellulose membrane, which was subsequently exposed to the appropriate the mixture of the primary antibody and its diluted buffer (1:1000) before detection using the horseradish peroxidase conjugated secondary anti-mouse or anti-rabbit antibody. All the nitrocellulose membranes were added Enhanced chemiluminescence (ECL) (Millipore, Darmstadt, Germany), and then visualized using the enhanced plus chemiluminescence assay kit (EMD Millipore, Billerica, MA, USA), according to the manufacturer's protocol. Primary and secondary antibodies used as described previously [16-18].

3.3. Survival Analysis

GEPIA2 performs survival analyses based on mRNA expression levels. The red blocks denote the higher and blue ones the lower risk. The blocks with darkened frames indicate statistical significance in prognostic analyses. This approach enabled us to screen for the prognostic impact of CAT in the different cancer types (http://gepia2.cancer-pku.cn/#index, accessed on 1 June 2022).

4. Results

4.1. CAT expression negatively correlates with LUAD invasion

In our previous studies revealed that overexpression of SOD2 enhanced cell migration, invasion, anchorage-independent soft-agar colony growth, and drug resistance via upregulating of FOXM1 expression, MMP2 expression, NFκB activation, and worse prognosis of LUAD [16-18].

In the precision medicine era, data from RNA-Seq of next-generation sequencing (NGS) tools

provides gene-expression databases, including Gene Expression Omnibus (GEO), Sequence Read Archive (SRA), and the Cancer Genome Atlas (TCGA) databases on the human gene transcriptome.

In this study, we further validated the relationship of SOD2, FOXM1, and MMP2 mRNA expression in an overview of the TCGA data within TIMER2.0 (http://timer.cistrome.org/) and the

Kaplan Meier survival analysis was completed by GEPIA2 (http://gepia2.cancer-pku.cn/#index).

In GEPIA online platform, 478 LUAD patients were classified into SOD2 high and low expression groups by median cutoff, and LUAD with high SOD2 in tumor tissues had significantly worse overall survival (OS) compared to those with low SOD2 levels (HR=1.4, P=0.035; Figure 1B).

In TIMER2.0 online service, SOD2 mRNA expression was positively correlated with FOXM1 and MMP2 mRNA expression (P<0.001 and R=0.269 for FOXM1 (Figure 1C) and P<0.001 and R=0.314 for MMP2 (Figure 1D)). The results of analysis of the large amount of expression data was consistent with our previous studies [16-18]. Subsequently, we further explored the downstream antioxidant of SOD2, CAT gene expression whether could be involved with LUAD progression and clinical prognosis. A panel of gradually increasing in invasiveness of lung adenocarcinoma cell lines from CL1-0 to CL1-5 were used to determine CAT expression that help us to explore the association between CAT and LUAD progression [25]. The results showed that CAT protein expression revealed gradual decreases from low to high invasiveness in the panel cells, whereas SOD2 protein expression was slightly increased in CL1-5 (Figure 1E). To further investigated the association of CAT, FOXM1, and MMP2 mRNA expression in an overview of the TCGA data within TIMER2.0 (http://timer.cistrome.org/), we found that CAT mRNA expression was negatively correlated with FOXM1 and MMP2 mRNA expression (P<0.001 and R=-0.45 for FOXM1 (Figure 1F) and P=0.244 and R=-0.0.051 for MMP2 (Figure 1G)). We further analyzed the percentage of CAT mutation, and the heatmap showed that CAT mutation rate was lower than 0.04% for each cancer type (Figure 1H).

We suggested that CAT could decrease SOD2-induced FOXM1 and MMP2 expression in LUAD.

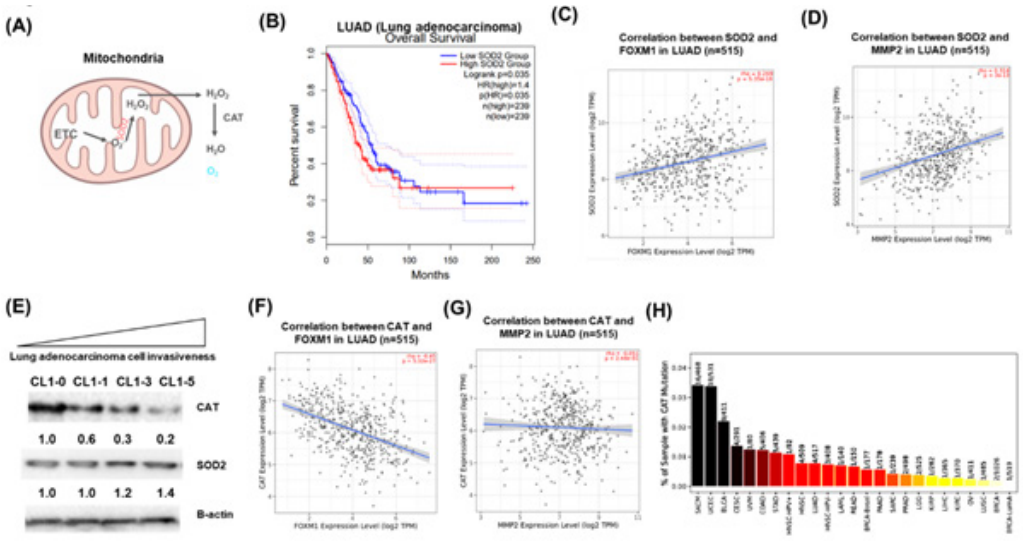

Figure 1: Validation of the relationship of SOD2, CAT, FOXM1, and MMP2 expression from TCGA datasets. (A) Schematic representation of H2O2 production increased by the interaction of SOD2 and superoxide anion (O2). Catalase which is often referred to as a major H2O2 scavenger throughout the cells. ETC stands for Electron Transport Chain. (B) Overall survival estimated for CAT expression using Kaplan-Meier analysis. (C) The correlations between SOD2 expression and FOXM1 expression in LUAD analyzed via TIMER2.0 database. (D) The correlations between SOD2 expression and MMP2 expression in LUAD analyzed via TIMER2.0 database. (E) Western blotting for SOD2 and CAT in a series gradually invasive potential cells CL1-0, CL1-1, CL1-3, and CL1-5. (F) The correlations between CAT expression and FOXM1 expression in LUAD analyzed via TIMER2.0 database. (G) The correlations between CAT expression and MMP2 expression in LUAD analyzed via TIMER2.0 database. (H) Analysis of somatic mutation rate of CAT in different cancer types.

4.2. Lower CAT expression is association with worse prognosis of BLCA, KIRC, LIHC, and LUAD

We further explored CAT whether has a tumor suppressor role in the multiple cancer types by Cancer Genome Atlas (TCGA) databases. The comprehensive analysis of CAT mRNA transcripts in different types of cancer and adjacent normal tissues in the TIMER2.0 database exhibited that the relative levels of CAT mRNA transcripts in different types of cancer were significantly lower than that in adjacent normal tissues apart from glioblastoma multiforme (GBN) (Figure 2A). We further compared the survival contribution of CAT mRNA expression in multiple cancer types, estimated using Mantel–Cox test. The results showed that low CAT mRNA expression had significantly worse prognosis of BLCA, KIRC, LIHC, and LUAD visualized by survival map (Figure 2B). The survival rates of the low CAT and high CAT groups were compared, finding a significant difference in overall survival between the two groups in BLCA (P=0.02, Figure 2C). The overall survival rate of high CAT was significantly higher than low CAT in KIRC (p<0.001, Figure 4D). The overall survival rate of high CAT was significantly higher than low CAT in LIHC (p=0.011, Figure 4E). High CAT of LUAD had longer survival time than that with low CAT (P=0.012, Figure 4F).

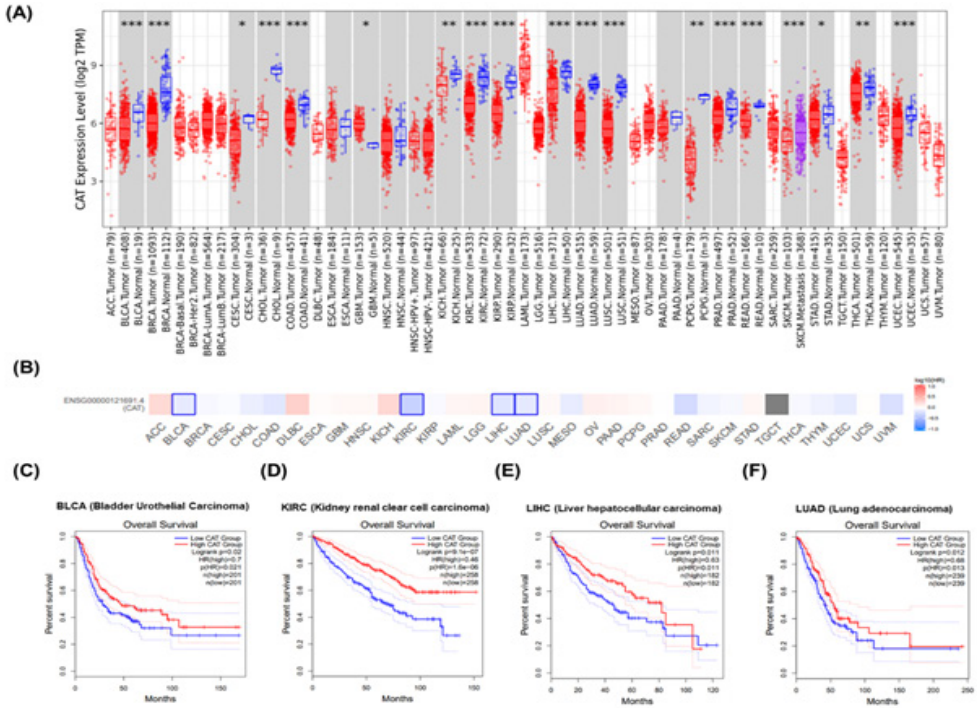

Figure 2: Low CAT expression was observed in different cancer types apart from GBM and associated with poor prognosis in BLCA, KIRC, LIHC, and LUAD. (A) Low CAT mRNA expression was found in several types of cancers. (B) A heat map to show the survival analysis result based on multiple cancer types. (C) Overall survival estimated for CAT expression using Kaplan-Meier analysis in BLCA. (D) Overall survival estimated for CAT expression using Kaplan-Meier analysis in KIRC. (E) Overall survival estimated for CAT expression using Kaplan-Meier analysis in LIHC. (F) Overall survival estimated for CAT expression using Kaplan-Meier analysis in LUAD.

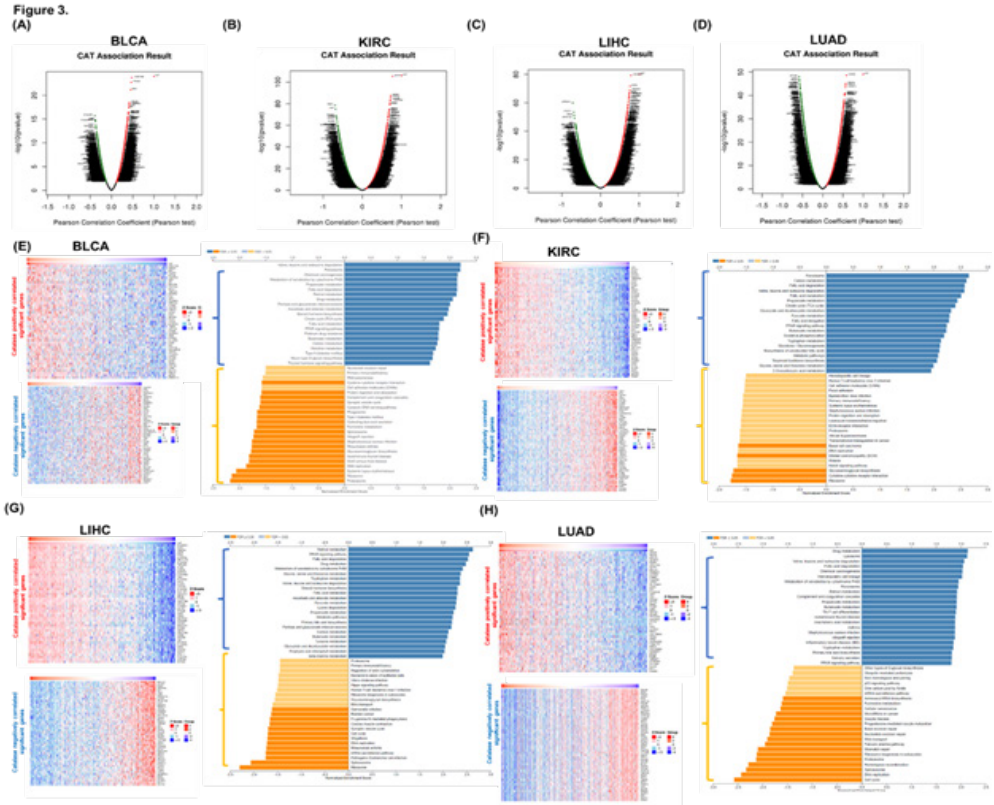

Figure 3: Identification of differentially expressed genes (DEGs) in TCGA BLCA, KIRC, LIHC, and LUAD mRNA expression profiling datasets using LinkedOmics. (A) Volcano plot of DEGs in TCGA BLCA dataset. (B) Volcano plot of DEGs in TCGA KIRC dataset. (C) Volcano plot of DEGs in TCGA LIHC dataset. (D) Volcano plot of DEGs in TCGA LUAD. (E) KEGG pathways enriched in CAT statistically correlated significant in BLCA. (F) KEGG pathways enriched in CAT statistically correlated significant in KIRC. (G) KEGG pathways enriched in CAT statistically correlated significant in LIHC. (H) KEGG pathways enriched in CAT statistically correlated significant in LUAD.

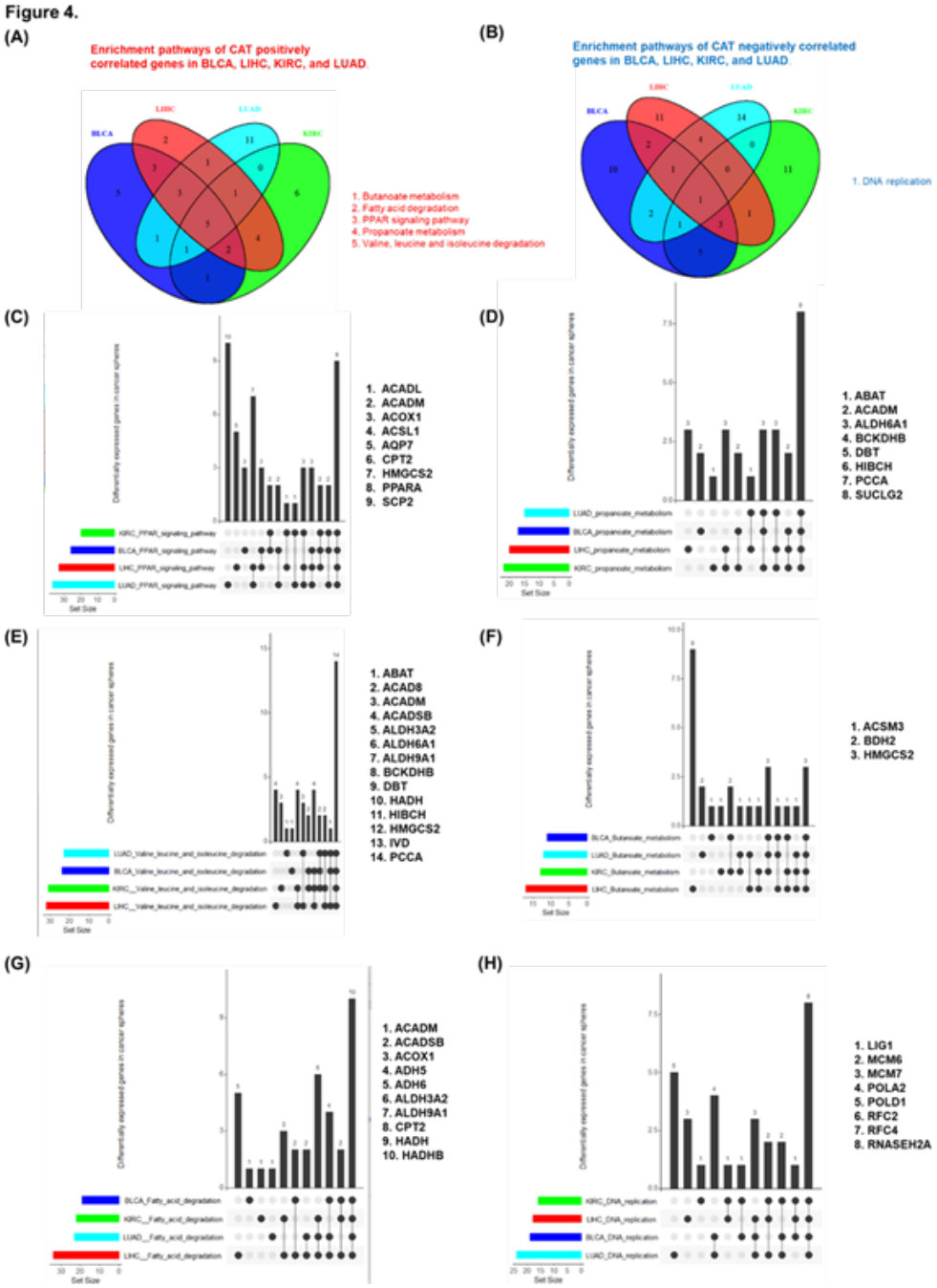

Figure 4: Intersection of CAT correlated KEGG pathways of BLCA, KIRC, LIHC, and LUAD.
(A) Venn diagram analysis of CAT positively correlated KEGG pathways of BLCA, KIRC, LIHC, (B) Venn diagram analysis of CAT negatively correlated KEGG pathways of BLCA, KIRC, LIHC, (C) Venn diagram analysis of DEGs in PPAR signaling pathway. (D) Venn diagram analysis of DEGs in propanoate metabolism. (E) Venn diagram analysis of DEGs in valine, and leucine and isoleucine degradation. (F) Venn diagram analysis of DEGs in butanoate metabolism. (G) Venn diagram analysis of DEGs in fatty acid degradation. (H) Venn diagram analysis of DEGs in DNA replication.

4.3. Enrichment analysis of the CAT gene co-expression profiles in BLCA, KIRC, LIHC, and LUAD

Based on the results, we suggested that CAT has tumor suppressor function in BLCA, KIRC, LIHC, and LUAD. To further understand the biological function of the transcriptional role of CAT in BLCA, KIRC, LIHC, and LUAD, the LinkedOmics database was used to predict genes associated with CAT. As shown in Figure 3A, there were 4,379 showed significantly negative correlations with CAT (red dots), and there were 4,784 revealed significantly negative correlations with CAT (green dots) in BLCA. In KIRC, a total of 5,278 genes were found to be significantly positively correlated with CAT (red dots), while 9,706 genes showed significantly negative correlations with CAT (green dots) (Figure 3B). A total of 5,007 genes were found to be significantly positively correlated with CAT (red dots), while 8,771 genes showed significantly negative correlations with CAT (green dots) in LIHC (Figure 3C). A total of 6,332 genes were found to be significantly positively correlated with CAT (red dots), while 5,763 genes showed significant-

ly negative correlations with CAT (green dots) in LUAD (Figure 3D). The top 50 genes that were significantly positively or negatively correlated with CAT are shown on a heat map, and KEGG enrichment pathways involved these CAT correlated genes (Figure 3F-3H). Therefore, we suggested that CAT expression could affect a large number of genes associated KEGG pathways.

4.4. The intersection KEGG enrichment pathways and their intersection genes in BLCA, KIRC, LIHC, and LUAD

Given the abundant CAT associated differently enriched pathways in BLCA, KIRC, LIHC, and LUAD, we wished to find common rules for these cancer types. All the pathways into CAT positively correlated genes and CAT negatively correlated genes, and there were five common pathways of CAT positively correlated genes in BLCA, LIHC, KIRC, and LUAD include butanoate metabolism, fatty acid degradation, PPAR signaling pathway, propanoate metabolism, and valine, leucine and isoleucine degradation (Figure 4A) and there was one common pathway of CAT negatively correlated genes in BLCA, LIHC, KIRC, and LUAD identified as DNA replication (Figure 4B). To further investigate the characteristics of identified differentially expressed genes (DEGs), we analyzed the intersection DEGs for each pathway in BLCA, LIHC, KIRC, and LUAD (Figure 4C-4H). Based on the above results, we suggested that CAT associated the upregulation of molecular metabolism and PPAR signaling pathway and the downregulation of DNA replication in BLCA, LIHC, KIRC, and LUAD.

4.5. Joint survival analysis of the five catalase-positive and one catalase-negative pathways enrichment-related gene sets in BLCA, KIRC, LIHC, and LUAD

We took the five catalase-positive and one catalase-negative pathways enrichment-related genes as gene sets and used GEPIA database to analyze the relationship between these gene sets and the prognosis of BLCA, KIRC, LIHC, and LUAD. The results revealed that the survival time of patients with upregulated genes of PPAR signaling pathway was significantly higher than that of patients with downregulated genes in KIRC ($P<0.001$, Figure 5A). Meanwhile, we performed the survival analysis in patients with BLCA showed that the expression of upregulated genes of propanoate metabolism was significantly higher than that of patients with downregulated genes ($P<0.001$, Figure 5B), the survival time of patients with upregulated genes of valine, leucine and isoleucine degradation was significantly higher than that of patients with downregulated genes in KIRC ($P<0.001$, Figure 5C), the survival time of patients with upregulated genes of butanoate metabolism was significantly higher than that of patients with downregulated genes in KIRC ($P<0.001$, Figure 5D), and the survival time of patients with upregulated genes of fatty acid degradation was significantly higher than that of patients with downregulated genes in KIRC and LIHC ($P<0.001$ and 0.043, respectively. Figure 5E). DNA replication, one catalase-negative pathway enrichment that the survival time of patients with upregulated genes was significantly lower than that of patients with downregulated genes in LIHC and LUAD ($P=0.0018$ and $P=0.0068$, Figure 5F).

4.6. CAT is positively correlated with FOXO3 expression in BLCA, KIRC, LIHC, and LUAD

Based on bioinformatics, we found that the CAT is located at chromosome 11p13, and an in-silico analysis with ALLGGEN_PROMO predicted fourteen putative FOXO3 binding sites in the CAT promoter region (Supplementary Figure 1A); thus, we speculated that FOXO3 might regulate CAT expression. Heatmap box was to explore the correlation between FOXO3 and CAT in various cancer types, and it gave the spearman's rho value was the degree of their positive correlation in all cancer types (Supplementary Figure 1B). Supplementary figure 1C-1F were revealed that CAT mRNA expression was positively correlated with FOXO3 mRNA expression.

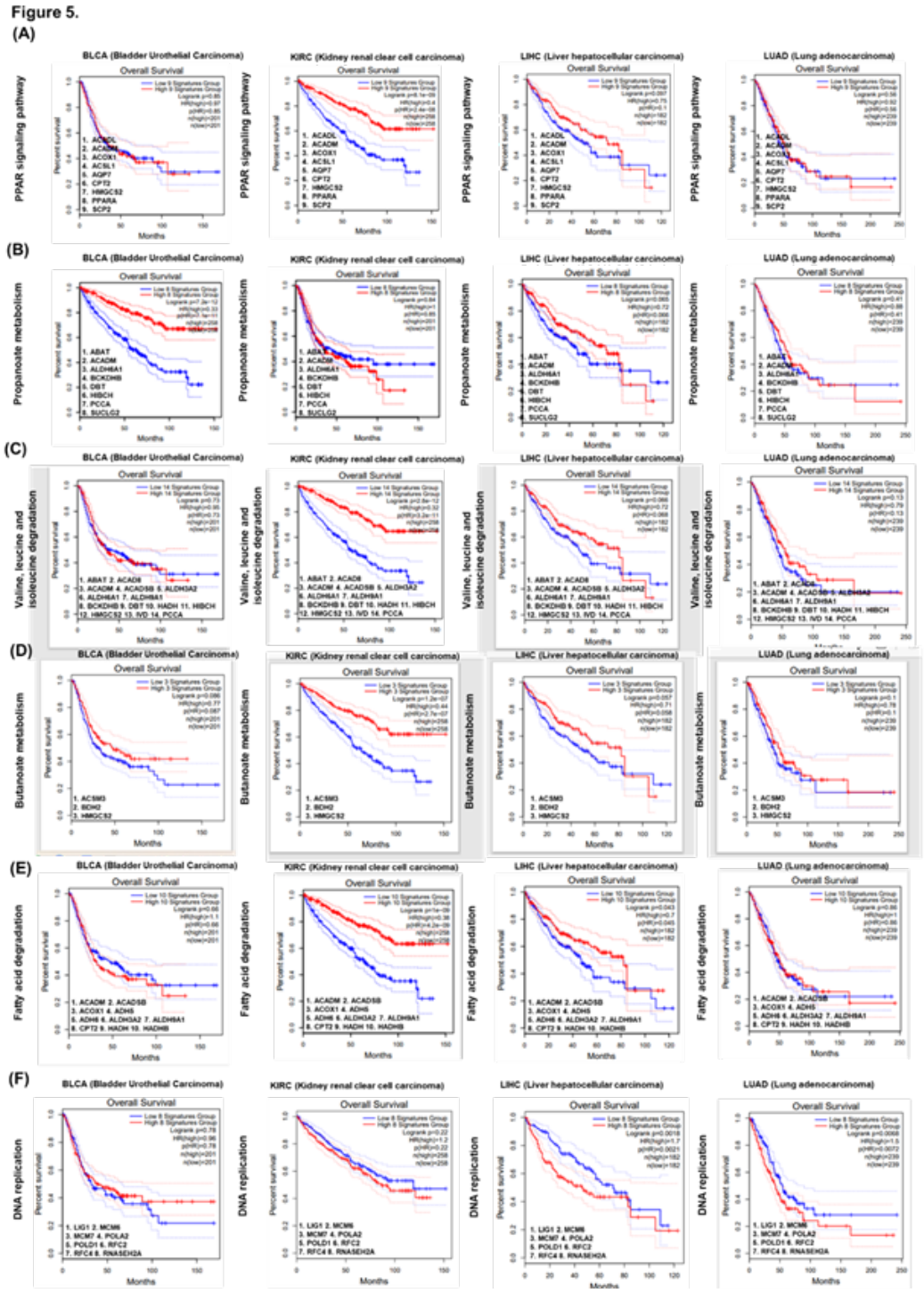

Figure 5: CAT associated gene signature to predict prognostic survival using GEPIA2 web server. (A) Kaplan–Meier plot of the nine-gene signature in PPAR signaling pathway. (A) Kaplan–Meier plot of the nine-gene signature in PPAR signaling pathway. (B) Kaplan–Meier plot of the eight-gene signature in propanoate metabolism. (C) Kaplan–Meier plot of the fourteen-gene signature in valine, leucine and isoleucine degradation. (D) Kaplan–Meier plot of the three-gene signature in butanoate metabolism. (E) Kaplan–Meier plot of the ten-gene signature in fatty acid degradation. (F) Kaplan–Meier plot of the ten-gene signature in DNA replication.

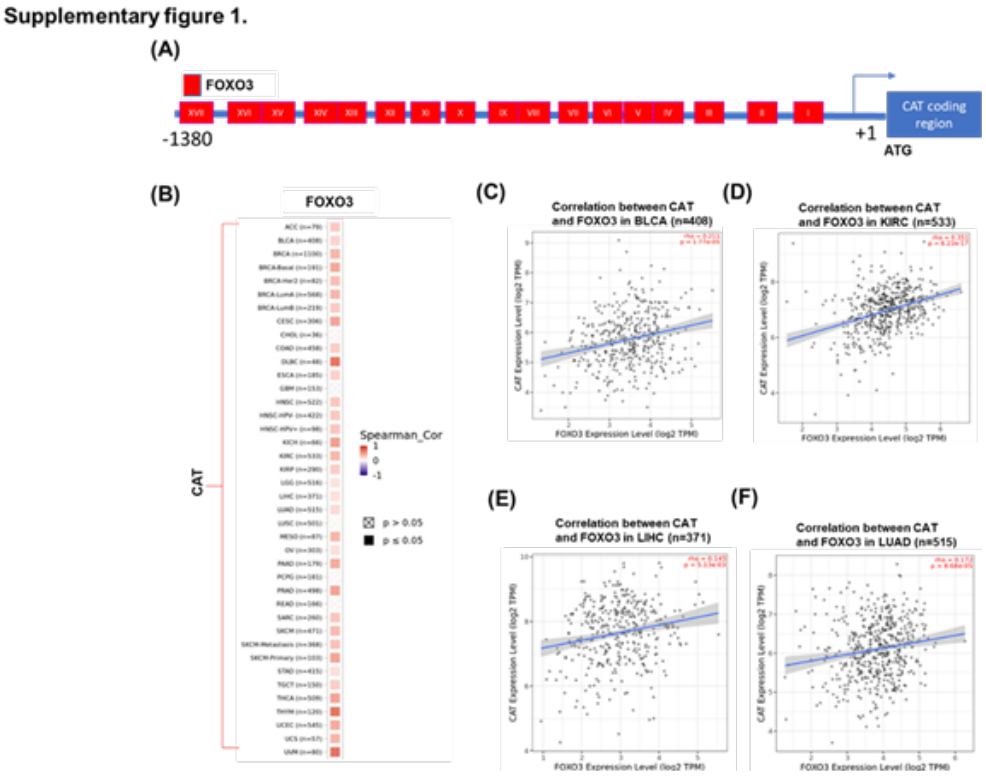

Supplementary Figure 1: FOXO3 was highly correlated with CAT mRNA expression. (A) Analysis of the putative transcription factor, FOXO3 on the CAT promoter. (B) A heat map to show the association between CAT an FOXO3 mRNA expression based on multiple cancer types. (C) The correlations between CAT expression and FOXO3 expression in BLCA analyzed via TIMER2.0 database. (D) The correlations between CAT expression and FOXO3 expression in KIRC analyzed via TIMER2.0 database. (E) The correlations between CAT expression and FOXO3 expression in LIHC analyzed via TIMER2.0 database. (F) The correlations between CAT expression and FOXO3 expression in LUAD analyzed via TIMER2.0 database.

5. Discussion

To continue our previous study on SOD2 in LUAD, we also found the positive relationship of SOD2, FOXM1, and MMP2 and the negative relationship of CAT, FOXM1, and MMP2 in TCGA LUAD data. CAT showed gradually decreases invasive potential in a series of CL1-0, CL1-1, CL1-3 and CL1-5 lung adenocarcinoma, but not SOD2 was slightly changed that could be due to these cells harbored p53 mutation (R248W) (Figure 1). p53-dependent oxidative stress and apoptosis in which p53-mediated up-regulation of SOD2 and glutathione peroxidase 1 (GPx), but not CAT [26]. However, we first proposed FOXO3 may upregulate CAT mRNA expression by binding its promoter (Supplementary Figure 1A). Forkhead transcription factors of the O class (FOXOs) factors regulate mitochondrial activity through inhibition of c-Myc function are key regulators of the cell cycle, apoptosis and response to hypoxia response [27] and also acts as the central regulator of cellular metabolic homeostasis [28].

Comprehensive survival analysis in TCGA datasets, high CAT expression had significantly longer survival time in BLCA, KIRC, LIHC, and LUAD; thus, we further investigated CAT-enriched pathways in these cancer types. By GSEA tools, butanoate metabolism, fatty acid degradation, PPAR signaling pathway, propanoate metabolism, valine, leucine and isoleucine degradation were positively common enrichment pathways and DNA replication was a negatively common enrichment pathway in CAT expression patients (Figure 4).

Additionally, we intersected common genes that served as a signature for each pathway to further examined whether it had an important role in clinical prognosis.

We took DNA replication related genes, including LIG1, MCM6, MCM7, POLA2, POLD1, RFC2, RFC4, and RNASEH2A as a signature had worse prognosis in LUAD patients with CAT expression.

We generalized pathways for better prognosis as propanoate metabolism in BLCA, butanoate metabolism, fatty acid degradation, PPAR signaling pathway, valine, leucine and isoleucine degradation in KIRC, and fatty acid degradation in LIHC.

Sodium propionate treatment inhibited cell growth in lung cancer cell lines by the regulation of survivin and p21 expression levels [29]. Gut microbiota-derived propionate reduced cancer cell proliferation through a cyclic adenosine monophosphate (cAMP) level-dependent pathway in LIHC [30]. Sodium butyrate selectively kills cancer cells and inhibits migration in colorectal cancer by increased reactive oxygen species (ROS) level and targeting thioredoxin-1 (Trx-1) [31] and decreases its own oxidation through inhibition of histone deacetylases in colorectal cancer (CRC) cells [32].

In xenograft animal models of lung cancer revealed decreased tumor growth and metastasis and a decrease of the incidence of lung cancer treated with PPARγ ligands [33]. Loss of branched-chain amino acid (BCAA), valine, leucine and isoleucine, are essential amino acids catabolism promotes tumor development and growth by enhancing mammalian target of rapamycin complex 1 (mTORCl) activity [34]. Fatty acid oxidation is associated with lower proliferation and better prognosis in in multiple tumor types [35]. We demonstrate CAT positively enriched pathways that the signatures of the common gene expression conferred better prognosis in multiple tumor types, these results are supported by the literature.

In summary, the result could be indicated the potential use of CAT or its downstream mediators to repress cancer metastasis. It will be important to develop optimal regimen of CAT or its downstream mediators of treatments in combination with conventional therapies of BLCA, KIRC, LIHC, and LUAD tumor to obtain the better benefits especially in the repression of metastasis.

6. Conclusions

In conclusion, although CAT is known to reduce H2O2 to water and molecular oxygen in multiple cancer types, its function is still rarely known. The results of the present study suggested that it could also function as an anticancer drug for the treatment of cancer, by enhancing butanoate metabolism, fatty acid degradation, PPAR signaling pathway, propanoate metabolism, valine, and leucine and isoleucine degradation and reducing DNA replication. Therefore, many hurdles must be cleared for CAT to be applicable in cancer treatment, and the present results suggest that CAT derived metabolites and genes for dietary therapy may help patients with cancer; however, in vivo studies are needed to further validate the effectiveness of CAT derived metabolites and genes.

7. Funding

This work was supported by Show-Chwan Memorial Hospital (grants SRD-111018, SRD-110030, SRD-109034, SRD-109035, and SRD107063) and Ministry of Science and Technology (MOST 106-2314-B-442-001-MY3 (C.P.Y.), MOST 109-2314-B-442-001 (C.P.Y.).

References

1. Sung, H. et al. Global Cancer Statistics 2020: GLOBOCAN Estimates of Incidence and Mortality Worldwide for 36 Cancers in 185 Countries. CA Cancer J Clin. 2021; 71: 209-249.
2. Liou, G. Y. & Storz, P. Reactive oxygen species in cancer. Free Radic Res. 2010; 44: 479-496.
3. Nakamura, H. & Takada, K. Reactive oxygen species in cancer: Current findings and future directions. Cancer Sci. 2021; 112: 3945-3952.
4. Han, D., Williams, E. & Cadenas, E. Mitochondrial respiratory chain-dependent generation of superoxide anion and its release into the intermembrane space. Biochem J. 2001; 353: 411-416.
5. Liochev, S. I. & Fridovich, I. The effects of superoxide dismutase on H2O2 formation. Free Radic Biol Med. 2007; 42: 1465-1469.
6. Ansenberger-Fricano, K. et al. The peroxidase activity of mitochondrial superoxide dismutase. Free Radic Biol Med. 2013; 54: 116-124.
7. Candas, D. & Li, J. J. MnSOD in oxidative stress response-potential regulation via mitochondrial protein influx. Antioxid Redox Signal. 2014; 20: 1599-1617.
8. Than, N. G. et al. Mitochondrial manganese superoxide dismutase mRNA expression in human chorioamniotic membranes and its association with labor, inflammation, and infection. J Matern Fetal Neonatal Med. 2009; 22: 1000-1013.
9. Subburayan, K., Thayyullathil, F., Pallichankandy, S., Cheratta, A. R. & Galadari, S. Superoxide-mediated ferroptosis in human cancer cells induced by sodium selenite. Transl Oncol. 2020; 13: 100843.
10. Veal, E. A., Day, A. M. & Morgan, B. A. Hydrogen peroxide sensing and signaling. Mol Cell. 2007; 26: 1-14.
11. Lennicke, C., Rahn, J., Lichtenfels, R., Wessjohann, L. A. & Seliger, B. Hydrogen peroxide - production, fate and role in redox signaling of tumor cells. Cell Commun Signal. 2015; 13: 39.
12. Rhee, S. G. Cell signaling. H2O2, a necessary evil for cell signaling. Science. 2006; 312: 1882-1883.
13. Connor, K. M. et al. Manganese superoxide dismutase enhances the invasive and migratory activity of tumor cells. Cancer Res. 2007; 67: 10260-10267.
14. Hempel, N., Carrico, P. M. & Melendez, J. A. Manganese superoxide dismutase (Sod2) and redox-control of signaling events that drive metastasis. Anticancer Agents Med Chem. 2011; 11: 191-201.
15. Miar, A. et al. Manganese superoxide dismutase (SOD2/MnSOD)/catalase and SOD2/GPx1 ratios as biomarkers for tumor progression and metastasis in prostate, colon, and lung cancer. Free Radic Biol Med. 2015; 85: 45-55.
16. Chen, P. M., Cheng, Y. W., Wu, T. C., Chen, C. Y. & Lee, H. MnSOD overexpression confers cisplatin resistance in lung adenocarcinoma via the NF-kappaB/Snail/Bcl-2 pathway. Free Radic Biol Med. 2015; 79: 127-137.
17. Chen, P. M. et al. MnSOD promotes tumor invasion via upregulation of FoxM1-MMP2 axis and related with poor survival and relapse in lung adenocarcinomas. Mol Cancer Res. 2013; 11: 261-271.
18. Chen, P. M. et al. Activation of NF-kappaB by SOD2 promotes the aggressiveness of lung adenocarcinoma by modulating NKX2-1-mediated IKKbeta expression. Carcinogenesis. 2013; 34: 2655-2663.
19. Kirkman, H. N. & Gaetani, G. F. Catalase: a tetrameric enzyme with four tightly bound molecules of NADPH. Proc Natl Acad Sci U S A. 1984; 81: 4343-4347.
20. Sepasi Tehrani, H. & Moosavi-Movahedi, A. A. Catalase and its mysteries. Prog Biophys Mol Biol. 2018; 140: 5-12.
21. Gebicka, L. & Krych-Madej, J. The role of catalases in the prevention/promotion of oxidative stress. J Inorg Biochem. 2019; 197: 110699.

22. Cho, M. Y. et al. Prognostic significance of catalase expression and its regulatory effects on hepatitis B virus X protein (HBx) in HBV-related advanced hepatocellular carcinomas. Oncotarget. 2014; 5: 12233-12246.

23. Tsai, J. Y., Lee, M. J., Dah-Tsyr Chang, M. & Huang, H. The effect of catalase on migration and invasion of lung cancer cells by regulating the activities of cathepsin S, L, and K. Exp Cell Res. 2014; 323: 28-40.

24. Flor, S. et al. Catalase Overexpression Drives an Aggressive Phenotype in Glioblastoma. Antioxidants (Basel). 2021; 10.

25. Chen, J. J. et al. Global analysis of gene expression in invasion by a lung cancer model. Cancer Res. 2001; 61: 5223-5230.

26. Hussain, S. P. et al. p53-induced up-regulation of MnSOD and GPx but not catalase increases oxidative stress and apoptosis. Cancer Res. 2004; 64: 2350-2356.

27. Ferber, E. C. et al. FOXO3a regulates reactive oxygen metabolism by inhibiting mitochondrial gene expression. Cell Death Differ. 2012; 19: 968-979.

28. Yadav, R. K., Chauhan, A. S., Zhuang, L. & Gan, B. FoxO transcription factors in cancer metabolism. Semin Cancer Biol. 2018; 50: 65-76.

29. Kim, K. et al. Propionate of a microbiota metabolite induces cell apoptosis and cell cycle arrest in lung cancer. Mol Med Rep. 2019; 20: 1569-1574.

30. Bindels, L. B. et al. Gut microbiota-derived propionate reduces cancer cell proliferation in the liver. Br J Cancer. 2012; 107: 1337-1344.

31. Wang, W. et al. Sodium Butyrate Selectively Kills Cancer Cells and Inhibits Migration in Colorectal Cancer by Targeting Thioredoxin-1. Onco Targets Ther. 2020; 13: 4691-4704.

32. Han, A., Bennett, N., Ahmed, B., Whelan, J. & Donohoe, D. R. Butyrate decreases its own oxidation in colorectal cancer cells through inhibition of histone deacetylases. Oncotarget. 2018; 9: 27280-27292.

33. Han, S. W. & Roman, J. Anticancer actions of PPARgamma ligands: Current state and future perspectives in human lung cancer. World J Biol Chem. 2010; 1: 31-40.

34. Ericksen, R. E. et al. Loss of BCAA Catabolism during Carcinogenesis Enhances mTORC1 Activity and Promotes Tumor Development and Progression. Cell Metab. 2019; 29: 1151-1165 e1156.

35. Aiderus, A., Black, M. A. & Dunbier, A. K. Fatty acid oxidation is associated with proliferation and prognosis in breast and other cancers. BMC Cancer. 2018; 18: 805.